Modelling the 'universal' dielectric response in heterogeneous materials using microstructural electrical networks

C. R. Bowen* and D. P. Almond

The frequency dependent conductivity and permittivity of a ceramic composite are modelled using electrical networks consisting of randomly positioned resistors and capacitors. The electrical network represents a heterogeneous microstructure that contains both insulating (the capacitor) and conductive regions (the resistor). To validate model results, a model ceramic conductor–insulator composite was designed consisting of a porous lead zirconate titanate impregnated with different concentrations of water. Excellent agreement between experimental and model data was achieved with a strong correlation with many other ceramics, glasses and composites. It is proposed that the 'universal' dielectric response of many materials is a consequence of microstructural heterogeneity. The modelling approach could be used as a simple and effective method for microstructural design of ceramics and other materials with tailored dielectric properties.

Keywords: Dielectric, Ceramic, Conductivity, Permittivity, Networks, Composite

Introduction

Heterogeneous materials containing phases that are conductive and dielectric (insulating) are present in a wide variety of man made materials and in nature. A striking observation is that many of these systems display a similar frequency dependent conductivity and permittivity, namely Jonscher's 'universal dielectric response' (UDR).[1] Examples of UDR behaviour in ceramic materials are in Fig. 1, which show the ac conductivity of an Al_2O_3–TiO_2 ceramic composite[2] and a doped zirconia at a variety of temperatures. At low frequencies the bulk (real) ac conductivity $\sigma(0)$ is frequency independent, but at higher frequencies the ac conductivity increases, following a power law behaviour such that

$$\sigma(\omega) \propto \omega^{n} \tag{1}$$

where ω is angular frequency ($2\pi f$) and n is typically $0{\cdot}6 < n < 1{\cdot}0$. The real part of the permittivity ε' can be expressed by a power law decay[3] such that,

$$\varepsilon' \propto \omega^{n-1} \tag{2}$$

The universality is considered incompatible with conventional Debye behaviour, the distribution of relaxation times (DRT) and stretched exponential approach,[4] Many body theories, fractal behaviour and hopping models have also been proposed.[5–7] Because the power laws are observed in a range of single crystal, polycrystalline and amorphous materials including ceramics, polymers, composites, wet cements, electronic and ionic conductors, it is important that any model must be able to account for the ubiquity of the UDR. For this reason there has been interest in the examination of the electrical response of random resistor–capacitor networks, which represent a heterogeneous microstructure consisting of conducting and insulating regions.[8–12] An example of a microstructure that can be regarded as a resistor–capacitor network is shown in Fig. 2, the Al_2O_3–TiO_2 ceramic composite in Fig. 1*a*, which consists of an intimate mixture of insulating Al_2O_3 (capacitor regions) and conducting TiO_2 (resistor regions). For the doped zirconia in Fig. 1*b*, the disorder is on a smaller scale whereby conducting oxygen vacancies are distributed in an insulating zirconia host. Other examples, which exhibit the UDR and have different scales of conductor–insulator heterogeneity, include rock–water and cement–water mixtures, Na β-alumina (sodium ions in conducting channels between insulating alumina blocks), conducting glasses, carbon loaded polymers, polymer blends, colloids, emulsions and biological tissues.

Typical response of microstructural electrical networks

A detailed analysis of the properties of random resistor–capacitor networks has been presented by Almond *et al.*[10,12] As a typical example, the electrical response of a network of randomly positioned resistors and

Materials Research Centre, Bath Institute for Complex Systems, Department of Mechanical Engineering, University of Bath, Claverton Down, Bath, BA2 7AY, UK

*Corresponding author, email c.r.bowen@bath.ac.uk

Published by Maney on behalf of the Institute
Received 18 April 2005; accepted 15 February 2005
DOI 10.1179/174328406X101328

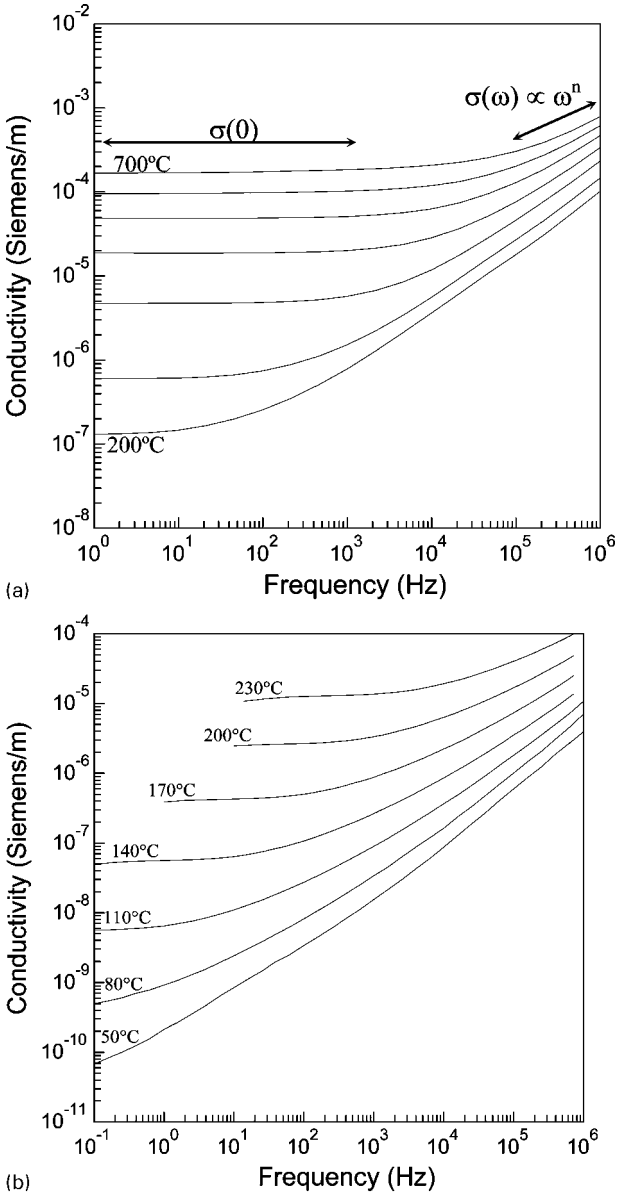

1 ac conductivity of *a* Al_2O_3 (insulator)–TiO_2 (conductor) composite[2] and *b* doped zirconia at various temperatures

capacitors, determined using circuit simulation software, is shown in Fig. 3. The network was a square 512 component lattice in which 60% of the components were 1 kΩ resistors and 40% were 1 nF capacitors.

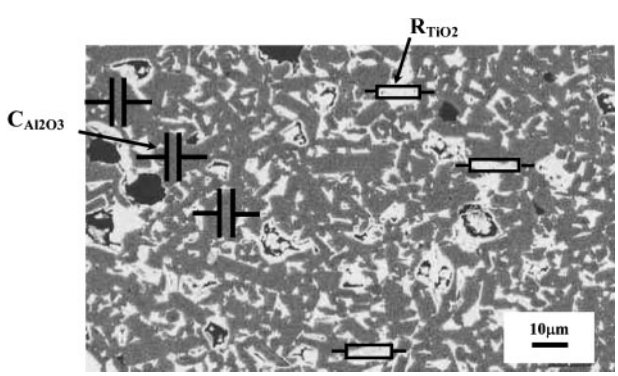

2 Microstructure of Al_2O_3–TiO_2 composite: grey phase corresponds to Al_2O_3 phase (capacitor, C_{Al2O3}); white region corresponds to TiO_2 (conductor, R_{TiO_2})[2]

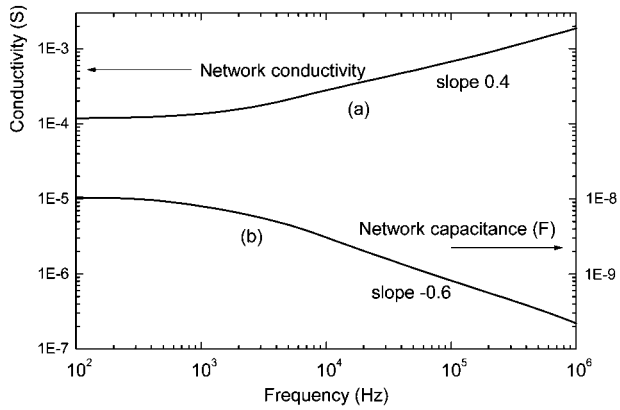

3 Simulations of *a* conductivity and *b* capacitance of 2D square network containing 512 randomly spaced components, 60% 1 kΩ resistors and 40% 1 nF capacitors: $R^{-1} \approx \omega C$ is satisfied at frequency of $1{\cdot}6 \times 10^5$ Hz

At low frequencies ($<10^3$ Hz) a frequency independent conductivity σ (0) is observed, as shown in Fig. 3*a*. In this frequency range current flows preferentially through the resistors and σ (0) corresponds to the one or more percolation paths of resistors across the network. At higher frequencies ($>10^4$ Hz) the resistor–capacitor network exhibits a frequency dispersion with clear power dependencies of conductivity and capacitance. The origin of the frequency dispersion can be determined by considering the response of the individual resistor and capacitor components with increasing frequency. The resistor conductivity R^{-1} is frequency independent; however the conductivity (admittance) of the capacitor ωC increases linearly with frequency. At a sufficiently high frequency the capacitor admittance is comparable with the resistor conductivity $R^{-1} \approx \omega C$ and in this frequency range both the resistors and capacitors now contribute to the overall network response. For the particular network in Fig. 3 the condition $R = \omega C$ is at $1{\cdot}6 \times 10^5$ Hz, because $R = 1$ kΩ and $C = 1$ nF. As the frequency is further increased the capacitor admittance continues to increase and the network ac conductivity rises with fractional powers of frequency (Fig. 3*a*) and the network capacitance falls as fractional powers of frequency (Fig. 3*b*). A comparison of the network response in Fig. 3 with the experimental data in Fig. 1 and equations (1) and (2) show that the electrical network response is qualitatively similar to the UDR.

Origin of power law response

To explain the characteristics of a complex network of resistor and capacitor components, it has been suggested[13,14] that a logarithmic mixing rule[15–17] be used. If a fraction α of the components are capacitors, the network complex conductivity σ^* and complex capacitance C^* are given by

$$\sigma^* = (i\omega C)^{\alpha}(R^{-1})^{1-\alpha} \text{ [hence } \sigma^* \propto \omega^{\alpha}\text{]} \quad (3)$$

$$C^* = \sigma^*/i\omega \text{ [hence } C^* \propto \omega^{\alpha-1}\text{]} \quad (4)$$

Equation (3) implies that the power law exponent for the conductivity equals the fraction of the network filled with capacitors ($\alpha = 0{\cdot}4$), and this is in good agreement with the network response in Fig. 3*a*, which exhibits a slope of 0·4. Similarly, the power law decrease in

network capacitance should have an exponent of $\alpha-1=-0{\cdot}6$, also matching the observed network simulation response in Fig. 3*b*. Such correlations between the power law dependencies and the network composition have been made with large numbers of resistor–capacitor networks of various compositions containing up to 32 768 components.[12]

Applying logarithmic mixing rule to heterogeneous materials

If the microstructure of a heterogeneous conductor–insulator material is to be modelled as a large network of conductive and capacitive islands, the resistor and capacitor values of equations (3) and (4) are replaced by the corresponding conductivity σ and permittivity ε, assuming the two phases have similar aspect ratios. The measurable bulk conductivity and relative permittivity predicted by the logarithmic mixing rule are now[10,11,14,15]

$$\sigma_{\text{meas}} = (\omega\varepsilon\varepsilon_0)^{\alpha}(\sigma)^{1-\alpha}\cos(\alpha\pi/2) \quad (5)$$

$$\varepsilon_{\text{meas}} = (\omega\varepsilon_0)^{\alpha-1}\varepsilon^{\alpha}\sigma^{1-\alpha}\sin(\alpha\pi/2) \quad (6)$$

where σ is the conductivity of the conducting phase, ε is the relative permittivity of dielectric phase, ε_0 is the permittivity of free space and α is the fractional volume of the material occupied by the insulating (dielectric) phase. Equations (5) and (6) indicate that $\sigma(\omega) \propto \omega^{\alpha}$ and $\hat{\varepsilon}(\omega) \propto \omega^{\alpha-1}$ and comparison with equations (1) and (2) implies that the power law exponent n, in the UDR is directly related to the volume fraction of dielectric phase α in a heterogeneous conductor–insulator material.

Model material design

In order to experimentally examine whether power law behaviour is the response of a microstructural electrical network, a composite system was designed with a microstructure containing a network of interconnected conductive and dielectric phases. The requirements for the model system were that

(i) it must be possible to independently characterise the conductor conductivity σ and dielectric relative permittivity ε
(ii) the dielectric volume fraction α must be known
(iii) the properties of each phase should, ideally be, frequency independent.

In addition, the power law dispersions must occur in an appropriate frequency range for electrical characterisation (typically <10 MHz). As previously described, power law dispersions are observed in the electrical networks when the admittance of the capacitor region ωC is similar to that of the resistor components R^{-1}. For a two phase material consisting of a conductor of conductivity σ, and an insulator of permittivity ε, this condition corresponds to $\sigma \approx \varepsilon\varepsilon_0\omega$ (assuming the two phases have similar volumes and shapes). Because relative permittivities of dielectrics are typically ~ 2 to ~ 3000, the conductivity of the conducting phase must be less than $\sim 10^{-1}$ S m^{-1}; which excludes metallic materials. The two materials selected to form a model test system were a porous (78% dense) lead zirconate titanate (PZT) ceramic as the insulator ($\varepsilon=1500$ for the dense material) and water as the conductive phase owing to its ease of impregnation into the PZT pore space and its sufficiently low conductivity ($\sim 0{\cdot}1$ S m^{-1}).

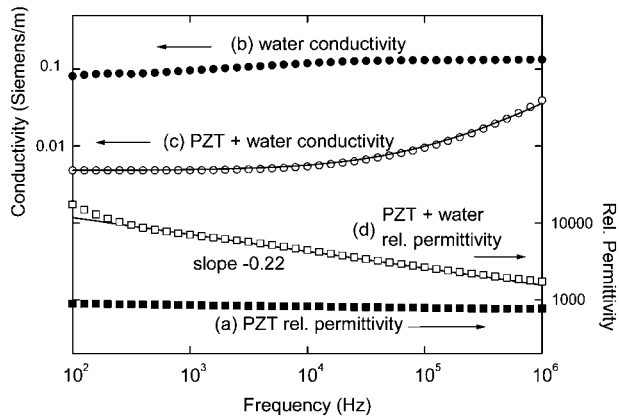

4 Measurements of *a* relative permittivity of porous PZT sample, *b* conductivity of water at equilibrium with immersed PZT fragments (*see* text), *c* conductivity and *d* relative permittivity of sample saturated with water

To manufacture the ferroelectric ceramic, PZT powder was mixed with a polymer additive that volatilised on sintering (1250°C) to form a porous PZT pellet. The pellet had a diameter of 10·5 mm, a thickness of 3 mm and a density 78% of the theoretical density of PZT. Silver paste electrodes were applied to the two circular faces and measurements were made using a Solatron 1260 impedance analyser with a Solatron 1296 dielectric interface. The measured relative permittivity of the porous PZT pellet, before the introduction of the water, is shown in Fig. 4*a* and is featureless across the frequency range shown and, as a result of the porosity, has a magnitude lower than that of the fully dense bulk material. Figure 4*b* shows the frequency dependence of the conductivity of the water that had been previously immersed in PZT for several days to simulate the condition of the water in the PZT pore space. The water conductivity is also featureless across the frequency range, apart from a fall in conductivity at low frequencies that is attributed to an electrode polarisation effect, commonly observed in ac measurements of all types of ionic conductor.

Experimental results of PZT water system

Frequency dependent permittivity and ac conductivity of saturated sample

After characterising the individual phases the pore space of the PZT ceramic was impregnated with water under vacuum. The resulting 78 vol.-%PZT–22 vol.-% water mixture represents a model conductor–insulator microstructure where the fraction of insulating phase α is 0·78 and, because $\varepsilon_{\text{PZT}}=1500$ and $\sigma_{\text{water}}=0{\cdot}13$ S m^{-1}, the condition $\sigma_{\text{water}}=\varepsilon_{\text{PZT}}\varepsilon_0\omega$ is satisfied at just over 1 MHz.

The frequency dependent ac conductivity and relative permittivity of the porous PZT sample saturated with water are shown in Fig. 4*c* and *d*. The ac conductivity shows a high frequency dispersion that is typical of both the UDR and the electrical network response. The relative permittivity is raised above the magnitude measured in the dry sample and it exhibits a clear power law decay with frequency. From equation (6), the

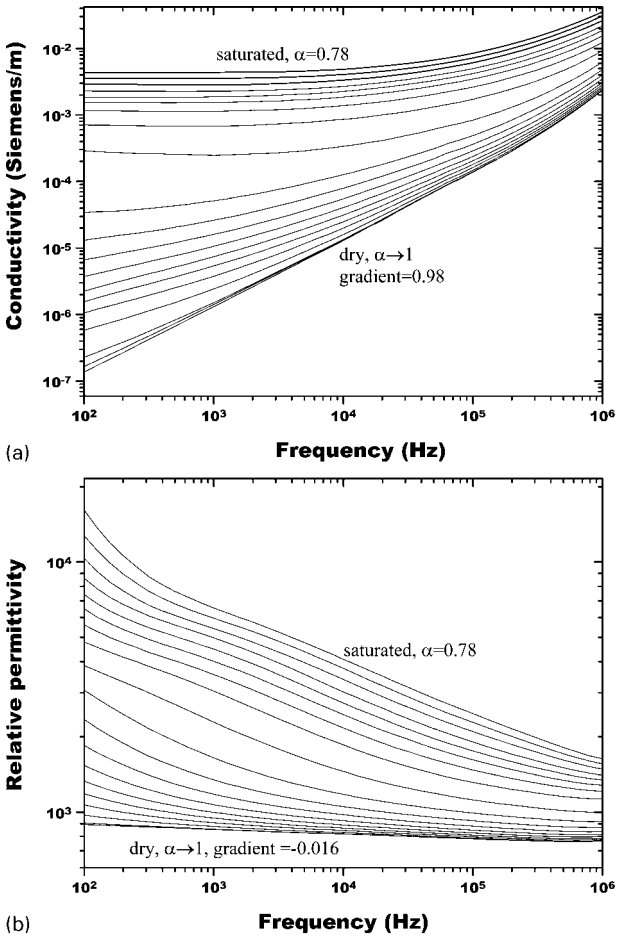

5 Measurements of *a* ac conductivity and *b* relative permittivity during drying of PZT–water mixture

power law exponent for the decrease in relative permittivity with frequency is $\alpha-1$. Because the volume fraction and density of the PZT was 78%, the slope of data in Fig. 4*d* is predicted to be –0·22. The line drawn in Fig. 4*d* is the system relative permittivity obtained from equation (6), setting $\alpha=0{\cdot}78$, using the bulk PZT relative permittivity ε of 1500 and a water conductivity of 0·13 S m^{-1}, indicated by the measurements shown in Fig. 4*b*. Since only materials properties have been used and there are no adjustable parameters, the overall agreement with the data is excellent.

The same properties were used in equation (5) to calculate the frequency dependent component of the ac conductivity, which was added to the percolation plateau, equation (7)

$$\sigma_{\text{meas}}=\sigma(0)+(\omega\varepsilon_{\text{PZT}}\varepsilon_0)^{\alpha}(\sigma_{\text{water}})^{1-\alpha}\cos(\alpha\pi/2) \qquad (7)$$

where $\sigma(0)=0{\cdot}0048$ S m^{-1} was used to generate the curve shown in Fig. 4*c*. Again, the overall agreement with the data is excellent.

Frequency dependent permittivity and ac conductivity during drying ($\alpha\rightarrow1$)

After the saturated measurements were made, the PZT was allowed to dry and measurements were made at regular intervals. Figure 5 shows the change in conductivity and permittivity as the composite composition varies from a fully saturated state (where $\alpha=0{\cdot}78$) to a dry state (where $\alpha\rightarrow1$). The magnitude of the frequency independent conductivity, $\sigma(0)$, decreased as the sample dried owing to the decrease in the amount of water contributing to the conductive percolation paths at low frequencies ($<10^4$ Hz) when $\sigma_{\text{water}}>\varepsilon_{\text{PZT}}\varepsilon_0\omega$. In addition, since the frequency dispersion occurs when the ac conductivity of the microstructural network (equation (5)) is comparable with σ (0), the frequency dispersion is observed at lower frequencies as the water content decreases and $\alpha\rightarrow1$.

There is a strong similarity between the ac conductivity results shown in Fig. 5*a* and that of the thermally activated ceramic conductors at different temperatures, as shown in Fig. 1*b*. The typical conductivity power law exponent for thermally active conductors ranges from 0·6–0·7 at high temperatures to ~1 at low temperatures. This correlates well with equation (5), because for a thermally activated conductor it would be expected that as $T\rightarrow0$, the fraction of conductor decreases and $\alpha\rightarrow1$. Dyre[5] stated that a 'universal' ac characteristic is that the power law regime is less temperature dependent than the low frequency plateau conductivity. This can be viewed as a consequence of the less temperature dependent dielectric phase contributing to the conductivity in the power law region (where $\omega C\geqslant\sigma$), while the low frequency σ (0) is dependent solely on the conductive phase. The high frequency power law regime in Fig. 5*a* is also less dependent on drying conditions for the same reason.

As the sample was dried and $\alpha\rightarrow1$, both the permittivity magnitude and gradient of the response in Fig. 5*b* decreased, as would be expected from equation (6). When the sample was fully dry the relative permittivity returned to the values shown in Fig. 4*a*, but the conductivity did not fall to zero. There was no observable σ (0) in the frequency range examined, but a conductivity rising linearly with frequency remained was present (*see* 'dry' data in Fig. 5*a*). The sample was heated in a vacuum furnace at 225°C to remove all traces of water but this had no effect on this residual conductivity. A very similar ac conductivity component was found in a fully dense sample of PZT that had not been exposed to water. Until now the dielectric region is assumed to be non-conductive, while the origin of this residual conductivity component is suggested by equations (5) and (6) in the limit of $\alpha\rightarrow1$

$$\sigma_{\text{meas}}\rightarrow\varepsilon\varepsilon_0\omega(1-\alpha)\pi/2 \qquad (8)$$

$$\varepsilon_{\text{meas}}\rightarrow\varepsilon\varepsilon_0^{\alpha-1}\omega^{\alpha-1} \qquad (9)$$

If the dielectric material is permeated by a small proportion $1-\alpha$ of conducting phase, equation (8) indicates that it will exhibit an ac conductivity rising linearly with frequency (the actual gradient of the 'dry' PZT curve in Fig. 5*a* is 0·98). An ac conductivity rising linearly with frequency has been widely reported[6,18] as a frequency independent dielectric loss, $\varepsilon''=\sigma(\omega)/\varepsilon_0\omega$ and this provides a possible explanation of this phenomenon, because when $\alpha\rightarrow1$, $\varepsilon'\rightarrow\varepsilon(1-\alpha)\pi/2$.

Prediction of power law dispersion in other heterogeneous systems

While the authors have established a case for the microstructural electrical network as a possible explanation of the UDR by employing a model ceramic–water

system, there remains the need to investigate the application of this model to a variety of other materials and composites. One indicator that this microstructural network approach is plausible is whether power law dispersions occur at frequencies where the admittance of the dielectric phase $\omega\varepsilon\varepsilon_0$ is similar to that of the conductive phase σ. A difficulty in making this assessment is that the actual conductivity of the conducting phase within a solid is often unknown. As an example, for the yttria doped zirconia in Fig. 1*b* the permittivity of the insulating ZrO_2 host phase is known but the effective conductivity of the oxygen vacancies is unknown. What is known is the low frequency plateau in conductivity σ (0), that is considered to be the dc conductivity of the material. In the PZT–water system an independent measurement of the conducting phase (water) conductivity has been made. The authors' data show the percolation conductivity of this water through the PZT pore system to be a factor $\sim$20 smaller than that of the actual water in the pores (compare the low frequency plateaus in Fig. 4*b* and *c*). The authors suggest that this factor is used to gain an order of magnitude estimate of the actual conductivity in other systems, i.e. in the equations above set $\sigma=20\sigma$ (0). This observation is in agreement with Archie's law[19] for the determination of dc conductivity of water saturated rocks, equation (10)

$$\sigma(0)=\sigma_{\text{water}}\phi^{\text{d}} \tag{10}$$

where σ_{water} is the conductivity of the water, ϕ is the porosity level and d is a constant (typically $\sim$2). From equation (10), using a PZT density of 78% ($\phi=0{\cdot}22$) and $d=2$, the water conductivity is estimated to be $20{\cdot}7\sigma$ (0).

Once the conductivity of the conductive phase has been estimated using $\sigma=20\sigma$ (0), the critical frequency at which the admittances of the two phases are equal needs to be determined. It can be seen from equation (5) that $\sigma_{\text{meas}}=\cos(\alpha\pi/2)\sigma$ when $\sigma\approx\varepsilon\varepsilon_0\omega$. As the measured conductivity power law exponent for many materials is found to lie in the range 0·6–0·8, $\cos(\alpha\pi/2)\approx0{\cdot}5$ and $\sigma_{\text{meas}}\approx0{\cdot}5\sigma\approx10\sigma(0)$ at the critical frequency. The frequency at which the ac conductivity has increased to $10\sigma(0)$ can be readily obtained from experimental data in the literature and then compared with the theoretical value calculated by setting $\omega\varepsilon\varepsilon_o=\sigma$, i.e. $f=20\sigma\,(0)/2\pi\varepsilon\varepsilon_o$. This introduces the host relative permittivity ε, a quantity that is usually available from independent measurements. Values of the measured and calculated frequencies, obtained from published data for a variety of heterogeneous ceramic, glass, polymeric and composite conductors exhibiting the UDR over a wide frequency range are listed in Table 1. The potential conductive and host insulating phases of these systems are also indicated. The experimental and calculated characteristic frequencies are compared in Fig. 6 and although exact matches are not expected, the overall correlation between the two frequencies is

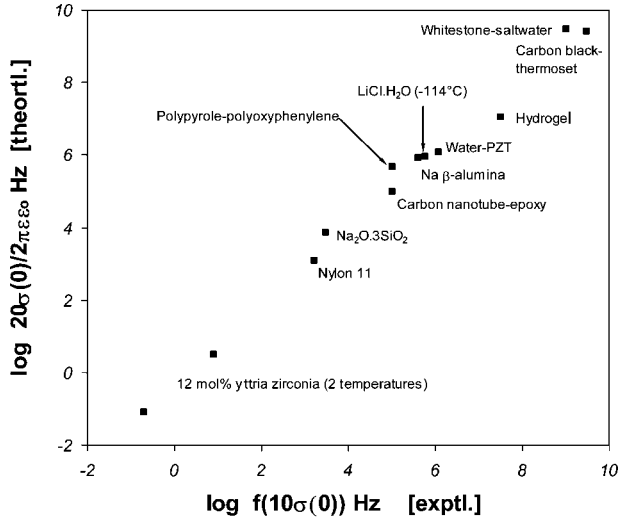

6 Correlation of theoretical characteristic frequency compared with experimental frequency

Table 1 Data used to compare experimental and theoretical critical frequencies

System	Conductive phase	σ (0), S m^{-1}	Host phase	Host ε	Frequency (10σ (0)) experimental, Hz	Frequency (20σ (0) /$2\pi\varepsilon\varepsilon_0$) theoretical, Hz
Water–PZT The present work	Water ($\sigma=0{\cdot}13$ S m^{-1})	$4{\cdot}8\times10^{-3}$	PZT	1500	$1{\cdot}2\times10^{6}$	$1{\cdot}16\times10^{6}$
Na β-alumina 113 K (Ref. 20)	Na ion channels	$2{\cdot}5\times10^{-5}$	Alumina	11	4×10^{5}	$8{\cdot}1\times10^{5}$
Na_2O–$3SiO_2$ glass (Ref. 21)	Na ions	4×10^{-8}	SiO_2	2	3×10^{3}	$7{\cdot}2\times10^{3}$
$LiCl.H_2O$ −114°C (Ref. 22)	Water	1×10^{-5}	LiCl	4	6×10^{5}	9×10^{5}
12 mol.-%Y_2O_3 zirconia (100°C)	Oxygen vacancies	2×10^{-10}	ZrO_2	22	8	3·2
60°C (Ref. 8)		5×10^{-12}		22	0·2	0·08
Carbon black in thermoset resin[23]	Carbon black	$2{\cdot}5\times10^{-2}$	Epoxy	3·5	3×10^{9}	$2{\cdot}6\times10^{9}$
Carbon nanotube (0·05 wt-%) in epoxy[24]	Carbon nanotube	$0{\cdot}9\times10^{-6}$	Epoxy	3·5	1×10^{5}	$9{\cdot}3\times10^{4}$
Poly(hydroxyethyl acrylate) hydrogel (PHEA)[25] (297 K, 0·32 g water/g)	Water	$0{\cdot}9\times10^{-4}$	PHEA	3	$3{\cdot}2\times10^{7}$	$1{\cdot}1\times10^{7}$
Nylon 11 (100°C)[26]	Protons and impurity ions	1×10^{-8}	Nylon 11	3	$1{\cdot}7\times10^{3}$	$1{\cdot}2\times10^{3}$
Polypyrole–polyoxyphenylene composite (150 K)[27]	Polypyrole conducting polymer	$3{\cdot}5\times10^{-6}$	Polyoxyphenylene	2·7	1×10^{5}	$4{\cdot}6\times10^{5}$
Whitestone–salt water[28]	Salt water ($\sigma=0{\cdot}93$ S m^{-1})	0·06	Whitestone	7·5	>1 GHz	$2{\cdot}9\times10^{9}$

strong. It is interesting to compare our PZT–water results with the whitestone–salt water data in Fig. 6. Because salt water has a high conductivity and whitestone has a small permittivity, it is not unexpected that higher frequencies (>1 GHz) are required to satisfy the condition $\sigma \approx \varepsilon\varepsilon_0\omega$ and observe the frequency dispersion.

Conclusions

The universal dielectric response has been related to the emergent response of random resistor–capacitor networks. The microstructure of heterogeneous materials is considered to form an electrical network and that it is the electrical response of the network that accounts for the observed power laws. Because microstructural heterogeneity is a common feature of many materials, such as the ceramics and composites of Table 1, this approach is also able to account for the ubiquity of the UDR. A simple formula to predict frequency dependent ac conductivity and permittivity is proposed in which all parameters (component conductivity, permittivity and composition) are independently testable. Excellent agreement with a model PZT–water system is observed, with a strong correlation with many other ceramics, glasses and composites (Table 1). The modelling approach could be used as a simple and effective tool for designing materials with tailored frequency dependent dielectric properties.

It is possible that many of the characteristics of the UDR can be related to the response of the microstructural electrical network, particularly at the critical frequency when the admittance of the host phase $\omega\varepsilon\varepsilon_o$ is comparable with that of the conducting phase in the material σ. The low frequency plateau, the power law regime and the linear frequency regime, which are observable in many heterogeneous materials, originate from its microstructural network. Indeed, it has been considered[18] that ac conductivity is best fitted by the sum of two power law components, such that $\sigma(\omega) = \sigma(0) + A\omega^{\alpha} + A'\omega$. The authors' interpretation is that the $\sigma(0)$ component corresponds to the low frequency plateau when currents percolate through the conductive phase ($\sigma \gg \omega\varepsilon\varepsilon_0$), the $A\omega^{\alpha}$ corresponds to intermediate frequencies when the currents flow through the whole microstructural network $\sigma \approx \omega\varepsilon\varepsilon_0$, and the final $A'\omega$ component corresponds to the high frequency, response when currents begin to percolate through the dielectric phase ($\sigma \ll \omega\varepsilon\varepsilon_0$).

References

1. A. K. Jonscher: *Nature,* 1975, **253**, 717.
2. R. Uppal: 'Effect of TiO_2 on the electrical conductivity of Al_2O_3', PhD thesis, University of Bath, Bath, UK, 2000.
3. V. Bobnar, P. Lunkenheimer, J. Henberger, A. Loidl, F. Lichtenberg and J. Mannhart: *Phys. Rev. Lett.*, 2002, **65**, 155115.
4. A. K. Jonscher: *IEEE Elec. Ins. Mag*., 1990, **6**, 16.
5. J. C. Dyre and T. B. Schrøder: *Rev. Mod. Phys*., 2000, **72,** 873.
6. A. Hunt: *Philos. Mag*., 2001, **81**, 875.
7. E. Tuncer, Y. V. Serdyuk and S. M. Gubanski: *IEEE Trans*., 2002, **9,** 809.
8. S. Jankowski: *J. Am. Ceram. Soc*., 1988, **71**, C176–C180.
9. B. Vainas, D. P. Almond, J. Luo and R. Stevens: *Solid State Ionics*, 1999, **126**, 65.
10. D. P. Almond and B. Vainas: *J. Phys. Condens. Matter,* 1999, **11,** 9081.
11. D. P. Almond and C. R. Bowen: *Phys. Rev. Lett.,* 2004**, 92**, 157601.
12. R. Bouamrane and D. P. Almond: *J. Phys. Condens. Matter,* 2003, **15**, 4089.
13. D. S. McLachlan, M. Blaszkiewiez and R. E. Newnham: *J. Am. Ceram. Soc*., 1990, **73,** 2187.
14. V. T. Truong and J. G. Teran: *Polymer,* 1995, **36**, 905.
15. K. Lichtenecker: *Z. Phys*., 1926, **27**, 115.
16. G. M. Tsangaris, G. C. Psarras and N. Kouloumbi: *Mater. Sci. Technol.,* 1996, 12, 533.
17. P. Drake and I. Youngs: *Mater. Sci. Technol.*, 2002, 18, 772.
18. A. S. Nowick, B. S. Lim and A. V. Vaysleyb: *J. Non-Cryst. Solids,* 1994, **172,** 1389.
19. G. E. Archie: *Trans. AIME*, 1942, **146,** 54.
20. R. J Grant, I. M. Hodge, M. D. Ingram and A. R. West: *Nature,* 1977, **266**, 42.
21. T. J. Higgins, P. B. Macedo and V. Volterra: *J. Am. Ceram. Soc*., 1972, **55,** 488.
22. C. T. Moynihan, R. D. Bressel and C. A. Angell: *J. Chem. Phys*., 1971, **55,** 4414.
23. L. J. Adriaanse, J. A. Reedijk, P. A. A. Teunissen, H. B. Brom, M. A. J. Michels and J. C. M Brokken-Zijp: *Phys. Rev. Lett.,* 1997, **78**,1755.
24. K. Bumsuk, J. Lee and Y. Insuk: *J. Appl. Phys*., 2003, **94**, 6724.
25. P. Pissis and A. Kyritsis: *Solid State Ionics,* 1997, **97**, 105.
26. R. M. Neagu, E. Neagu, N. Bonanos and P. Pissis: *J. Appl. Phys*., 2000, **88**, 6669.
27. J. Aguilar-Hernandez and K. Ptoje-Kamloth: *J. Phys. D,* 2001, **34D**, 1700.
28. W. E. Kenyon: *J. Appl. Phys*., 1984, **58**, 3153.